Hindawi
Journal of Advanced Transportation
Volume 2022, Article ID 8946794, 13 pages
https://doi.org/10.1155/2022/8946794

Research Article

Combined Phase Design Model for Multileg Roundabout Intersections

Chengyuan Mao, Qin Wang, Wenjiao Xu, Xin Cheng, Shengde Yang, and Peiran Li

College of Engineering, Zhejiang Normal University, Jinhua 321000, Zhejiang, China

Correspondence should be addressed to Chengyuan Mao; maocy@zjnu.cn

Received 4 April 2022; Revised 25 June 2022; Accepted 23 August 2022; Published 3 October 2022

Academic Editor: Indrajit Ghosh

Multileg roundabout intersections are widely used in urban areas worldwide. However, its traffic organization and signal control are very complicated in the case of large traffic flow, and the signal optimization methods for conventional intersections are not suitable for applying directly to roundabouts due to the complexity of the operating process. Therefore, many scholars have focused on dedicated signal timing schemes for roundabouts, especially through tuning key parameters such as signal cycle and green light time. However, research and applications regarding variable phases at roundabouts are quite rare. To address this gap, this paper analyzes the traffic flow characteristics and capacity of multileg roundabouts and proposed a combined phase design model to achieve the maximum utilization of road capacity at roundabouts, which can generate the optimal phase scheme based on real-time traffic data. The feasibility of the combined phase design model is verified by a case study in Jinhua, China. The results indicate that the proposed combined phase design model can improve the applicability of actuated signal control and the reasonableness of signal timing for multileg roundabouts and thus further improve the roundabout efficiency.

1. Introduction

A roundabout is one of the most common intersection forms of a modern road network and has the advantages of simple organization and fewer conflicts. Compared to non-signalized crossing intersections, roundabouts can substantially reduce traffic crashes and delays in the free flow state [1]. However, when a roundabout tends to saturate, traffic flow from each approach would obtain the right of way simultaneously, which results in the traffic flows' conflict and blocks the roundabout from obtaining maximum efficiency/capacity. Therefore, signal control can be introduced to address this issue and further improve roundabout efficiency [2].

Although fixed-time signal control or multiperiod fixed-time control is a common signal control approach, it is only suitable for intersections with stable traffic. For multileg roundabouts with unstable traffic, actuated signal control has been adopted to adapt to the fluctuation of traffic flow.

However, the application of actuated signal control in roundabouts has failed to achieve satisfactory performance for a long time since roundabout traffic flows are too complex. According to the observation, the actuated signal control is not effective. Therefore, extensive research efforts from various traffic scholars have been put into this field, which can be mainly classified into the following two categories: roundabout capacity and roundabout signal control.

In terms of roundabout capacity, there are three capacity calculation methods for roundabouts: gap acceptance theory, empirical regression model, and interleaving theory. The gap acceptance theory [3, 4] mainly analyzes the capacity of each approach to the roundabout. The empirical regression model [5–7] calculates the roundabout capacity by establishing a regression equation between the entry capacity and the circulating flow. The interleaving theory [8] takes the maximum traffic in the weaving section as the roundabout capacity according to the short board effect.

As for roundabout signal control, it is mainly divided into control parameter optimization and phase optimization. Some existing studies considered optimizing parameters such as green time [9, 10] and signal cycle [11–13] to improve the traffic efficiency of roundabouts. Shiri and

Maleki [14] optimized the maximum green light time parameter based on fuzzy control to better adapt to traffic demand changes. Ma et al. [15] proposed a method that can optimize lane markings and signal timing simultaneously to obtain maximum capacity, minimum cycle time, and minimum delay at roundabouts. However, the above signal control research does not consider the optimization of the phase. In the study of phase optimization, Jiang et al. optimized the design of phases, such as considering the phase of the coordinated signal in the circulating lanes and the approach carriageways [16], as well as quantitatively analyzing a certain type of phase—the left-turn phase [17]. Wu et al. [18] introduced a new phase into the actuated signal control, which could control the traffic flow of reversed left-turns so as to maximize the utilization rate of both the left-turn lanes and the reversed lanes. Xia and Xu [19] took each phase as the research object and proposed a phase coordination control method based on the negotiation game optimization model. Considering the different functions of lanes, Nei and Ma [20] established a lane-based intersection lane function and signal phase optimization model. Shen et al. [21] proposed a method of traffic phase combination and signal timing optimization based on the improved K-Medoids algorithm. Liang et al. [22] proposed an overlapping phase-based signal control logic and a bus priority control algorithm under two-way signal coordination on arterial roads.

It is found from the above literature that two typical zones of a roundabout—either the approach zone or the weaving zone—were selected for capacity calculation. The roundabout capacity is calculated based on the vehicle characteristics of these zones. However, the above-mentioned existing studies did not consider the roundabout as a whole and ignored the negative impacts of other bottleneck areas on the traffic efficiency of the roundabout. Moreover, each structural part of the roundabout would also affect the overall capacity. As for the studies on roundabout signal control, most of the existing studies still use fixed phase schemes, which lack consideration of dynamic changes in traffic demand (unstable traffic fluctuations and complex turning) at roundabouts. The current research on phase optimization is mostly based on the relatively stable phase, which cannot be adjusted actively with the real-time traffic flow, so the control effect is compromised. The research on the signal phase of roundabouts is relatively rare, and most of them focus on only a specific traffic flow state, which make them difficult to be widely used.

To solve these problems, this study attempts to consider and analyze each structural component of the roundabout and calculate the capacity according to the characteristics of different zones. Then, a combined phase design model is proposed to maximize the roundabout capacity utilization by enabling dynamic phasing scheme changes based on traffic demand.

2. Roundabout Traffic Flow Characteristics and Capacity Analysis

A signal phase specifies a combination of one or more traffic movements receiving the right of way simultaneously during a signal interval [23]. Phase design is constrained by the structure, traffic flow characteristics, and traffic capacity of the intersection.

2.1. Roundabout Structure. A roundabout consists of the following structures: a central island, a circulating lane, an approach carriageway, a departure carriageway, and a splitter island. The different geometric parameters of these structures and the different interactions among vehicles would lead to very different vehicle operation characteristics, which would affect the traffic efficiency of the roundabout. Therefore, the division of multileg roundabouts into different areas is crucial [24].

In a typical roundabout, there are five areas with different traffic flow features: the approach area, the merge area, the lane-changing area, the diverge area, and the departure area. As Figure 1 shows, the five areas of the carriageway/leg i of a roundabout are respectively represented by $A_i, B_i, C_i, D_i,$ and E_i.

Compared to straight roads, traffic flow operations in weaving zones would face shorter lane-changing distances and more complex conflicts because the traffic flow must merge, lane-change, and divert within such short distances and must slow down or even stop to wait for the right of way, which forms a bottleneck area. Therefore, in order to improve the roundabout's operational efficiency, this paper first analyzes the capacity of each bottleneck area.

2.2. Capacity. Usually, the capacity of the approach area or departure area is similar to that of the straight road, and it is much larger than the capacity of the merge area, the lane-changing area, or the diverge area. Therefore, only the capacities of the latter three areas will be discussed in the following sections.

Assuming $T_{i,k}$ is the traffic volume generated from carriageway i and goes to the carriageway k (pcu/h). $T_i = \sum_{k=1}^{N} T_{i,k}$ is the total traffic volume generated from the approach of carriageway i. Then, the capacity of the merge area, the lane-changing area, and the diverge area can be acquired as follows.

2.2.1. Merge Area. The actual capacity of the merge area can be calculated as follows [25]:

$$Q_{Bi} = \sum_{x=1}^{y} \frac{3600}{h_x}, \tag{1}$$

where Q_{Bi} is the actual capacity of merge area B_i (pcu/h); y is the number of circulating lanes; h_x is the average time headway between vehicles for saturated traffic conditions in circulating lane $x(s)$.

When calculating the traffic volume in a particular merge area, the traffic flows originating from each approach should be considered, but only part of them will pass through that merge area. Take the merge area B_1 (See Figure 1) as an example. Traffic flows generated from carriageway 1 will all pass through the merge area B_1, and traffic flows generated from carriageway 2 will also pass through B_1 except for those

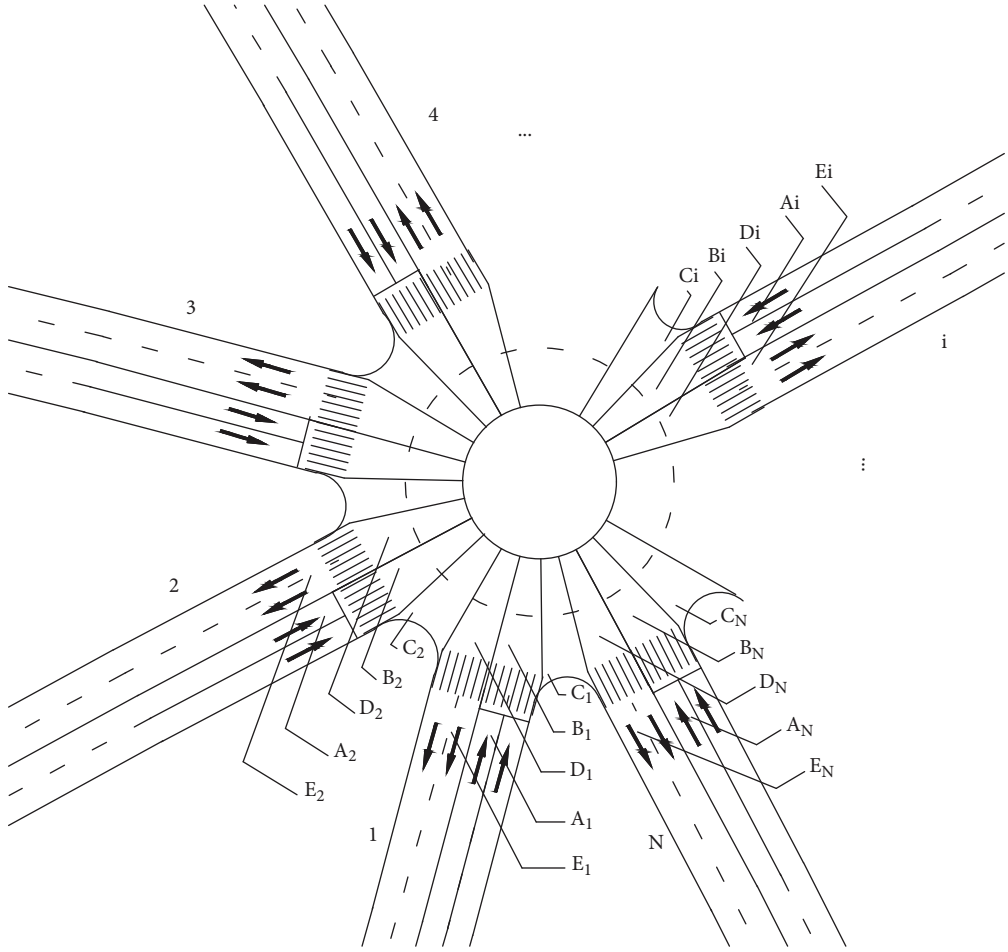

Figure 1: Structure of a multileg roundabout.

leaving the roundabout via departure carriageway 1. Similarly, it is easy to derive that traffic flows generated from the carriageway N will pass through the merge area B_1 except for those leaving the roundabout via departure carriageway 1, 2, 3, . . ., and $N - 1$. Therefore, the traffic volume of the merge area B_1 is $\sum_{i=1}^{N}\sum_{k=i}^{N} T_{i,k}$. Assume that m is an integer, one can also obtain the traffic volume of the merge area B_i as

$$T_{Bi} = \sum_{m=i}^{N+i-1}\sum_{k=m}^{N+i-1} T_{m,k}. \tag{2}$$

2.2.2. Lane-Changing Area. In this area, the actual road capacity is closely related to the drivers' lane-changing behaviour, and it can be calculated as follows [26]:

$$Q_{Ci} = \begin{cases} v_{fi}\rho_i, 0 \le \rho_i \le \dfrac{\rho_{ai}}{1+\epsilon_i} \\ \\ \dfrac{\rho_{ai}}{\rho_{bi}-\rho_{ai}} v_{fi} \dfrac{\rho_{bi} - \rho_i(1+\epsilon_i)}{1+\epsilon_i}, \dfrac{\rho_{ai}}{1+\epsilon_i} \le \rho_i \le \dfrac{\rho_{bi}}{1+\epsilon_i} \end{cases}, \tag{3}$$

where Q_{Ci} is the actual capacity of the lane-changing area C_i (pcu/(h·ln)); v_{fi} is the free flow speed in the area C_i (km/h); ρ_i is the total density of the lane-changing traffic density and nonlane-changing traffic density (pcu/(km·ln)); ρ_{ai} is the critical density of the area C_i (pcu/(km·ln)); ρ_{bi} is the jam density (pcu/(km·ln)); ε_i is the lane-changing intensity of area C_i, which can be calculated as follows:

$$\varepsilon_i = \begin{cases} 0, & \rho_i \le \rho_{ai}, \\ \\ \dfrac{2 - 2\rho_i/\rho_{bi}}{15 + 2\rho_i/\rho_{bi}}, & \rho_i \ge \rho_{ai}. \end{cases} \tag{4}$$

Since area C_i is adjacent to area B_i, it is easy to derive that the traffic volume T_{Ci} equals the traffic volume T_{Bi}, which is expressed as follows:

$$T_{Ci} = T_{Bi}. \tag{5}$$

2.2.3. Diverge Area. To simplify the combined phase design model, we assume that the drivers have completed lane changes before entering the diverge area. In addition, by assuming that the roundabout has a dedicated right-turn lane, vehicles in the diverge area will not conflict with each other. Therefore, the maximum actual capacity Q_{Di} that passes through the diverge area D_i is the actual capacity

leaving the lane-changing area C_{i+1} which can be calculated using

$$Q_{Di} = Q_{Ci+1}. \tag{6}$$

After analyzing the traffic flow in each direction, it was found that the vehicles passing through area C_{i+1} were flowing to the area D_i. As such, the traffic volume T_{Di} can be acquired as follows:

$$T_{Di} = T_{Ci+1}. \tag{7}$$

3. Combined Phase Design Model

3.1. Design Principles. For the nonoversaturated state, this paper proposed the following five regulations for the combined phase design model:

(1) Each roundabout approach must set a green light at least once in a cycle.

(2) The number of phases in a cycle should be kept as small as possible.

(3) The traffic volume in each roundabout area must not exceed its capacity.

(4) The red lights should be as few as possible in a single phase. Set red lights preferentially for approaches with smaller traffic volumes.

(5) The queuing vehicles in the corresponding approach shall be released within one green light.

3.2. Mathematical Expression

3.2.1. Traffic Volume. According to the definition of T_i in section "Capacity," the traffic volume at the multileg roundabout is as follows:

$$T = [T_1, T_2, \ldots, T_i, T_{i+1}, \ldots, T_N]^T = \left[T_{i,k}\right]_{N\times N}, \tag{8}$$

where i is the order of approach carriageways; k is the order of departure carriageways; N is the total number of approaches.

3.2.2. Phase. In this paper, we use 1 to indicate that the approach carriageway is set green light and 0 to indicate that the approach carriageway is set red/amber light, which means

$$U_{i,j} = \begin{cases} 1, & \text{when Approach } i \text{ set green light in Phase } j, \\ 0, & \text{when Approach } i \text{ set red/amber light in Phase } j, \end{cases} \tag{9}$$

where j is the order of phase and $U_{i,j}$ refers to the light state of approach i in phase j.

If we further define U_j as the light states of all the approach carriageways in phase j, the phase matrix U can be expressed as

$$U = \left[U_1, U_2, \ldots, U_j, U_{j+1}, \ldots, U_M\right]^T = \left[U_{i,j}\right]_{M\times N}, \tag{10}$$

where M is the total number of phases expressed as $M = C_N^0 + C_N^1 + C_N^2 + \ldots + C_N^{N-1} = 2^N - 1$.

3.2.3. Phase Scheme. Since the signal phase scheme is different combination of phases in one cycle, it can be described as follows:

$$p = \{p_1, p_2, \ldots, p_l, p_{l+1}, \ldots, p_L\}, \tag{11}$$

where l is the order of phase scheme. Taking v for a full array, it is an integer and takes values in the range of $[1, 2^N - 1]$. We take the value of $2^N - 1$ as an example, and the number of arrays is $A_{2^N-1}^{2^N-1}$. However, it should be noted that {1, 2, ..., $2^N - 1$}, {2, 3, ..., $2^N - 1$, 1}, {3, 4, ..., $2^N - 1$, 1, 2}, ..., {$2^N - 1$, $2^N - 2$, ..., 2, 1} all refer to the same phase scheme. Hence, the actual number of phase schemes is $A_{2^N-1}^{2^N-1}/2^N - 1$. Thus, the total number of possible phase schemes L is described as follows:

$$L = \frac{A_{2^N-1}^1}{1} + \frac{A_{2^N-1}^2}{2} + \ldots + \frac{A_{2^N-1}^{2^N-1}}{2^N - 1}. \tag{12}$$

3.2.4. Passable Traffic Volume. The traffic that can pass in one cycle is

$$T_V = \sum_{j=1}^{P}\sum_{i=1}^{N}\sum_{k=1}^{N}\left(T_{i,k}\cdot U_{i,j}\right), \tag{13}$$

where P is the order of phases in a cycle; T_V is the traffic that can pass in one cycle.

3.3. Model Formulation. According to the design principles introduced in section "Design Principles," the proposed combined phase design model is described as follows:

$$\max T_V = \sum_{j=1}^{P}\sum_{i=1}^{N}\sum_{k=1}^{N}\left(T_{i,k}\cdot U_{i,j}\right),$$
$$s.t.\begin{cases} T_{Bi} \le Q_{Bi} \\ T_{Ci} \le Q_{Ci} \\ T_{Di} \le Q_{Di} \\ \sum_{j=1}^{p}\sum_{i=1}^{N} U_{i,j} \ge N \\ N \ge Z\left(U_{j+1} - U_j\right) \ge 1 \\ \min P \end{cases}. \tag{14}$$

3.4. Explanation of Model Conditions

3.4.1. Capacity of Each Roundabout Area. The traffic volume in each roundabout area must not exceed its capacity, which corresponds to

$$\begin{aligned} T_{Bi} &\le Q_{Bi}, \\ T_{Ci} &\le Q_{Ci}, \\ T_{Di} &\le Q_{Di}. \end{aligned} \tag{15}$$

3.4.2. Restriction of Setting Green Light. Each roundabout approach should set a green light at least once in a cycle, which is equivalent to

$$\sum_{j=1}^{p} \sum_{i=1}^{N} U_{i,j} \ge N. \tag{16}$$

3.4.3. The Front Phase and Following Phase. To keep the signal cycle as short as possible, when setting up the next phase, at least one of the approach carriageways that was set as a red light in the previous phase should be set green, which means

$$N \ge Z\left(U_{j+1} - U_j\right) \ge 1, \tag{17}$$

where $Z(U_{j+1} - U_j)$ is the number of times accumulated when $U_{i,j} = 1$.

3.4.4. Number of Phases. As the number of phases increases, the loss time will also increase. Therefore, the number of phases P in a cycle should be kept as small as possible.

$$\min P. \tag{18}$$

3.5. Model Objectives. The optimization objective of the combined phase design model is to make more vehicles T_V pass through the roundabout in a single signal cycle, which is

$$\max T_V = \sum_{j=1}^{P} \sum_{i=1}^{N} \sum_{k=1}^{N} \left(T_{i,k} \cdot U_{i,j}\right). \tag{19}$$

3.6. Solution Algorithms. Since there are $2^N - 1$ phase combination schemes at roundabouts with N legs, the number of phase schemes will increase exponentially with the number of legs. In addition, given that we also need to consider the variability of traffic flow directions and the real-time demand of phase schemes, it is impractical to solve the phase schemes manually. Instead, we use computer tools, such as Python, VB, and so on, to solve the schemes.

Due to the finiteness of the phase schemes, we use the Python programming language to build and solve the combined phase design model. Specifically, the programming flowchart is shown in Figure 2, and the detailed steps are also listed as follows:

Step 1 Input the traffic volume of each direction at the roundabout and the parameters related to the actual capacity of each area

Step 2 Combine all approach carriageways of the roundabout to generate M phases

Step 3 Calculate the actual capacity and traffic volume of each merge area, lane-changing area, and diverge area at phase j

Step 4 If the results from Step 3 for phase j meet the conditions formulated by equations (15), save phase j or else go to Step 5

Step 5 Let $j = j + 1$, if $j > 2^N - 1$, go to Step 6 or else return to Step 3

Step 6 Use all saved phases as Phase Scheme Set U. Arrange the alternative phases and remove any identical phases to obtain a Phase Scheme Set p

Step 7 If Phase Scheme p_l meets the conditions formulated by equations (16)–(18), save p_l to p and calculate T_C of p_l or else go to Step 8

Step 8 Let $l = l + 1$, if $l > L$, go to Step 9 or else return to Step 7

Step 9 Comparing T_C of all phase schemes in p, the phase scheme satisfying equation (19) is the model output

4. Case Study

4.1. Current Situation. The Hou-Cheng-Li Rd./Bei-Shan Rd. Roundabout (hereinafter referred to as the target roundabout) is a five-leg roundabout located on the 1st Ring Road of Jinhua. The west of the roundabout leads to the Jinhua Railway Station and the West Jinhua Highway Station, the north leads to Guang-fu Hospital, and the south leads to the high-density residential community and a thriving business district. In a word, the roundabout is a key node of the local road network.

At present, the roads in Jinhua city mostly use green wave control. However, the target roundabout not only has morning and evening peaks but also has significant traffic flow fluctuations throughout the day. Therefore, even the green wave control scheme did not work well at the roundabout.

Table 1 and Figure 3 summarize the current situation of the target roundabout.

4.2. Traffic Survey. The traffic flow data for the target roundabout was provided by the Traffic Police Brigade of Jinhua and selected for the morning peak period (7:00 am to 9:00 am). Table 2 summarizes the traffic volume for 2 cycles at the roundabout. As shown in Figure 4, the current timing scheme has two phases, and the signal cycle is 75 seconds.

4.3. Capacity Calculation. According to section "Capacity," by substituting the mean value of the saturation headway into equation (1), the actual capacity Q_{Bi} of each merge area is obtained, and by substituting the free flow velocity v_{fi}, the total density ρ_i, the critical density ρ_{ai}, the jam density ρ_{bi}, and the lane-changing intensity ε_i into equations (3) and (6), the actual capacity Q_{Ci} of each lane-changing area and the actual capacity Q_{Di} of each diverge area are obtained, which are shown in Table 3.

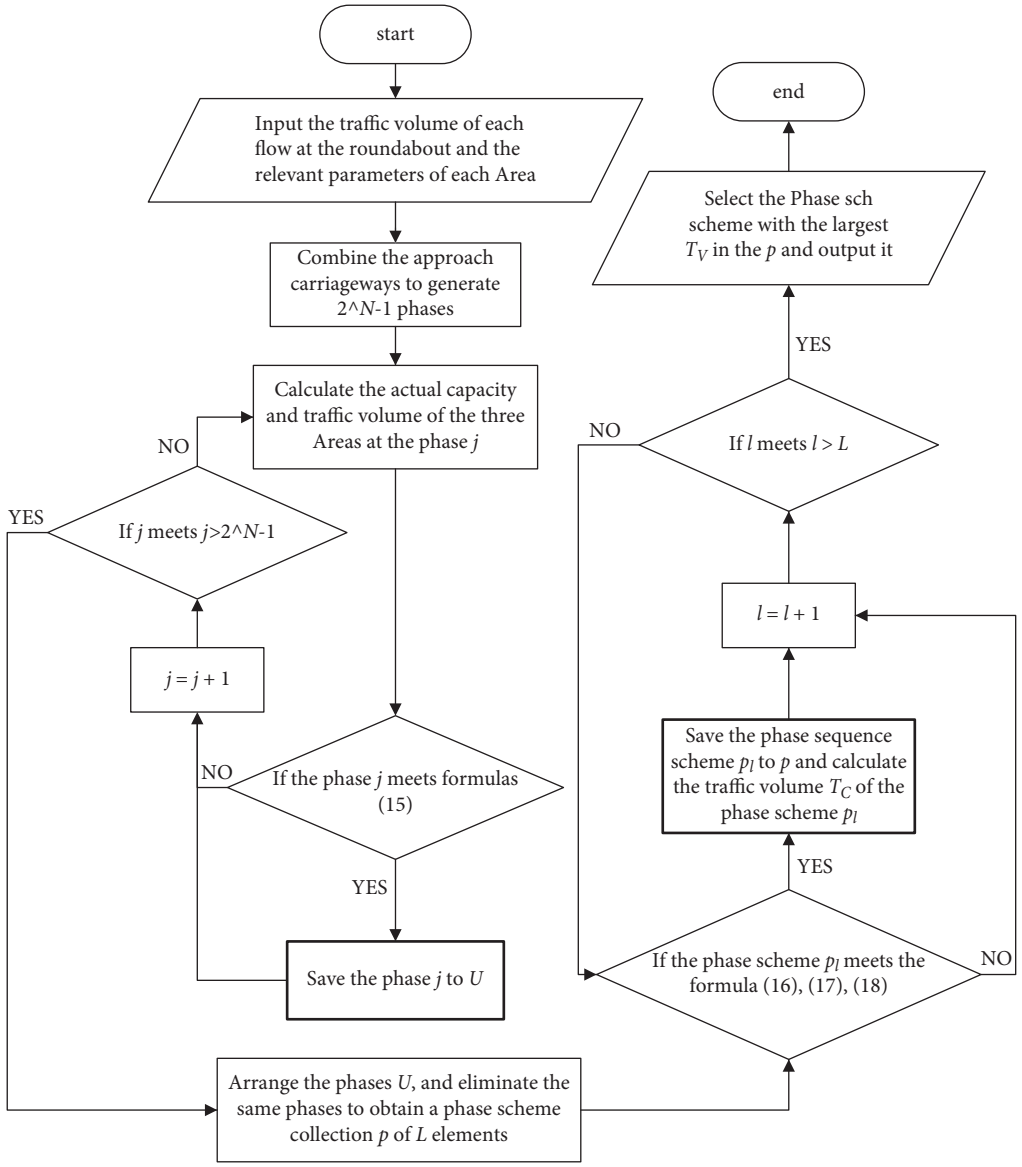

Figure 2: Programming flow chart of the combined phase design model.

Table 1: The number of lanes on each leg.

Approach	Huan-Cheng West Rd.	Bei-Shan Rd.	Huan-Cheng North Rd.	Feng-Ting West Rd.	Hou-Cheng-Li rd.
Number of approach lanes	3	2	3	1	2
Number of departure lanes	3	3	3	1	2

Note: the Huan-Cheng West Rd. is marked as approach carriageway 1, and Bei-Shan Rd., Huan-Cheng North Rd., Feng-Ting West Rd., and Hou-Cheng-Li Rd. are labeled in clockwise direction as approach carriageway 2, 3, 4, and 5, respectively. The circulating lane closest to the central roundabout is marked as circulating lane 1, and the outer circulating lanes are marked as circulating lanes 2, 3, and 4 in sequence.

Meanwhile, the following 3 points should be noted.

4.3.1. Merge Area. The video survey method was used to derive the saturation headway for each merging area, as shown in Table 4.

4.3.2. Lane-Changing Area. According to the statistical analysis of the on-site traffic data at the target roundabout, the parameter values of free flow velocity v_{fi}, total density ρ_i, critical density ρ_{ai}, jam density ρ_{bi}, and lane-changing intensity ε_i are shown in Table 5.

Other parameters can be expressed as

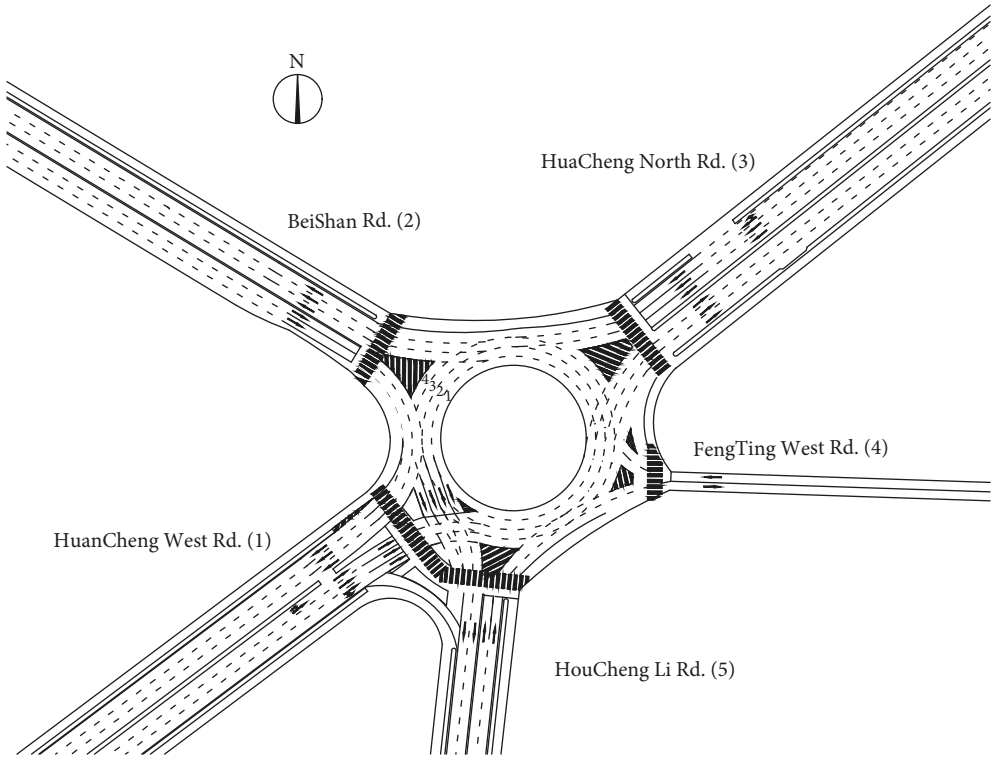

Figure 3: Current traffic organization of the roundabout.

Table 2: Traffic volume (pcu/h).

Approach no.	Cycle no.	1	2	3	4	5	Approach traffic volume
1	1	44	214	623	26	82	989
	2	52	243	678	25	95	1093
2	1	256	33	81	22	334	726
	2	271	29	71	26	320	717
3	1	425	315	57	21	184	1002
	2	364	293	35	13	179	884
4	1	6	16	3	0	3	28
	2	5	12	4	0	3	24
5	1	84	168	190	18	19	479
	2	70	161	195	12	15	453

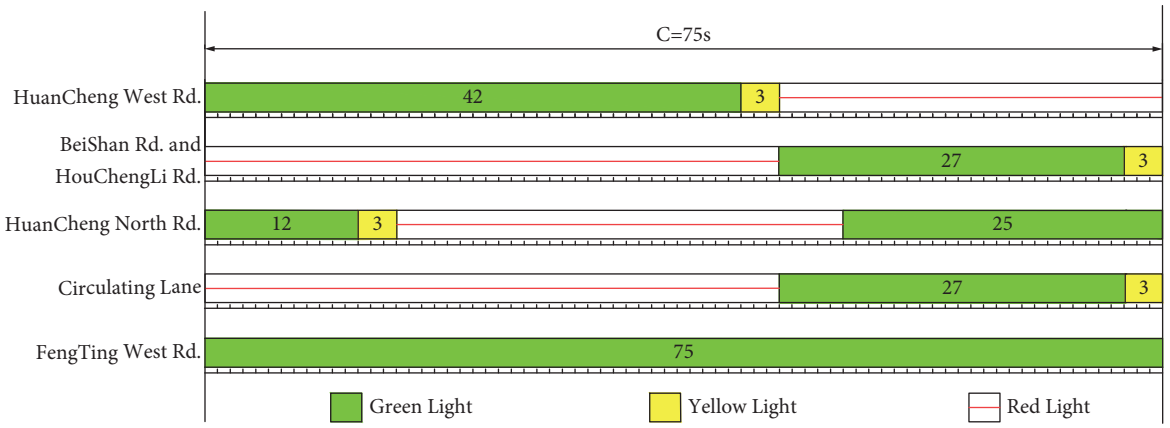

Figure 4: Current signal timing scheme.

Table 3: The actual capacity of each approach carriageway of the target roundabout.

Approach no.	Cycle no.	1	2	3	4	5
Q_{Bi} (pcu/h)	1	3174	3174	3174	3174	3174
	2	3164	3164	3164	3164	3164
Q_{Ci} (pcu/h)	1	967	1151	3006	1647	2417
	2	967	1442	3029	1785	2272
Q_{Di} (pcu/h)	1	1151	3006	1647	2417	967
	2	1442	3029	1785	2272	967

Table 4: Average saturated headway for circulating lanes in the merge area.

Parameters	Cycle no.	Circulating lanes 1	Circulating lanes 2	Circulating lanes 3	Circulating lanes 4
Average saturated headway (s)	1	3.78	4.30	4.85	5.60
	2	3.72	4.38	4.89	5.64

Table 5: Various parameter values of the lane-changing areas of the target roundabout.

Parameters	Cycle no.	1	2	3	4	5
v_{fi} (km/h)	1	24	25	29	26	28
	2	23	24	28	27	27
ρ_i (pcu/(km·ln))	1	93	92	82	89	85
	2	93	90	82	89	86
ρ_{ai} (pcu/(km·ln))	1	62	62	62	62	62
	2	63	63	63	63	63
ρ_{bi} (pcu/(km·ln))	1	100	100	100	100	100
	2	100	100	100	100	100
ε_i	1	0.0083	0.0095	0.0216	0.0131	0.0180
	2	0.0083	0.0119	0.0216	0.0131	0.0167

Note: the length of the lane-change area L_{lc}, passing time T_{lc}, traffic volume Q_{lc}, saturation traffic volume Q_{slc}, and distance headway D_{lc} are obtained through the camera survey. The D_{lc} is 9.95 m. ε_i is obtained from equation (4).

$$\begin{aligned} v_{fi} &= \frac{L_{lc}}{T_{lc}}, \\ \rho_i &= \frac{Q_{lc}}{L_{lc}}, \\ \rho_{ai} &= \frac{Q_{slc}}{L_{lc}, s}, \\ \rho_{bi} &= \frac{1000}{D_{lc}}. \end{aligned} \tag{20}$$

4.3.3. Diverge Area. The source of the various parameters of the diverge area is the same as the lane-changing area. According to equation (6), the various parameter values of the diverge area D_i are shown in Table 6.

4.4. Phase Design. In cycle 1, based on Step 1 of the flowchart in Figure 2, we input the traffic volume of each flow at the target roundabout and the relevant parameter values of each area into equation (14). In addition, since Huan-Cheng West Rd. has dedicated U-turn and right-turn lanes, the corresponding traffic flows ($T_{1,1}$ and $T_{1,5}$) will not pass through each merge area, lane-changing area, and diverge area. As such, $T_{1,1}$ and $T_{1,5}$ are set as 0.

According to Steps 3–6 of the flowchart, the Phase Scheme Set U that meets the capacity constraints of each area can be obtained as

$$U = \begin{bmatrix} 0 & 0 & 1 & 1 & 1 \\ 1 & 0 & 0 & 1 & 1 \\ 0 & 1 & 0 & 1 & 1 \\ 1 & 0 & 0 & 0 & 1 \\ 0 & 1 & 0 & 0 & 1 \\ 0 & 0 & 1 & 1 & 0 \\ 1 & 0 & 0 & 1 & 0 \\ 0 & 0 & 1 & 0 & 1 \\ 0 & 1 & 0 & 1 & 0 \\ 0 & 0 & 0 & 1 & 1 \\ 0 & 0 & 1 & 0 & 0 \\ 1 & 0 & 0 & 0 & 0 \\ 0 & 1 & 0 & 0 & 0 \\ 0 & 0 & 0 & 0 & 1 \\ 0 & 0 & 0 & 1 & 0 \end{bmatrix}. \tag{21}$$

Then, according to Steps 7-8 of the flowchart, the Phase Scheme Set p is formulated as follows:

Table 6: Various parameter values of the diverge areas of the target roundabout.

Parameters	Cycle no.	1	2	3	4	5
v_{fi} (km/h)	1	25	29	26	28	24
	2	24	28	27	27	23
ρ_i (pcu/(km·ln))	1	92	82	89	85	93
	2	90	82	89	86	93
ρ_{ai} (pcu/(km·ln))	1	62	62	62	62	62
	2	63	63	63	63	63
ρ_{bi} (pcu/(km·ln))	1	100	100	100	100	100
	2	100	100	100	100	100
ε_i	1	0.0095	0.0216	0.0131	0.0180	0.0083
	2	0.0119	0.0216	0.0131	0.0167	0.0083

$$\left\{ \begin{array}{l} \begin{bmatrix} 0 & 0 & 1 & 1 & 1 \\ 1 & 0 & 0 & 1 & 1 \\ 0 & 1 & 0 & 1 & 1 \end{bmatrix}, \begin{bmatrix} 0 & 0 & 1 & 1 & 1 \\ 1 & 0 & 0 & 1 & 1 \\ 0 & 1 & 0 & 0 & 1 \end{bmatrix}, \begin{bmatrix} 0 & 0 & 1 & 1 & 1 \\ 1 & 0 & 0 & 1 & 1 \\ 0 & 1 & 0 & 1 & 0 \end{bmatrix}, \begin{bmatrix} 0 & 0 & 1 & 1 & 1 \\ 1 & 0 & 0 & 1 & 1 \\ 0 & 1 & 0 & 0 & 0 \end{bmatrix}, \\ \begin{bmatrix} 0 & 0 & 1 & 1 & 1 \\ 0 & 1 & 0 & 1 & 1 \\ 1 & 0 & 0 & 0 & 1 \end{bmatrix}, \begin{bmatrix} 0 & 0 & 1 & 1 & 1 \\ 0 & 1 & 0 & 1 & 1 \\ 1 & 0 & 0 & 1 & 0 \end{bmatrix}, \begin{bmatrix} 0 & 0 & 1 & 1 & 1 \\ 0 & 1 & 0 & 1 & 1 \\ 1 & 0 & 0 & 0 & 0 \end{bmatrix}, \begin{bmatrix} 0 & 0 & 1 & 1 & 1 \\ 1 & 0 & 0 & 0 & 1 \\ 0 & 1 & 0 & 0 & 1 \end{bmatrix}, \\ \begin{bmatrix} 0 & 0 & 1 & 1 & 1 \\ 1 & 0 & 0 & 0 & 1 \\ 0 & 1 & 0 & 1 & 0 \end{bmatrix}, \begin{bmatrix} 0 & 0 & 1 & 1 & 1 \\ 1 & 0 & 0 & 1 & 1 \\ 0 & 1 & 0 & 0 & 0 \end{bmatrix}, \begin{bmatrix} 0 & 0 & 1 & 1 & 1 \\ 0 & 1 & 0 & 0 & 1 \\ 1 & 0 & 0 & 1 & 0 \end{bmatrix}, \begin{bmatrix} 0 & 0 & 1 & 1 & 1 \\ 0 & 1 & 0 & 0 & 1 \\ 1 & 0 & 0 & 0 & 0 \end{bmatrix}, \\ \begin{bmatrix} 0 & 0 & 1 & 1 & 1 \\ 1 & 0 & 0 & 1 & 0 \\ 0 & 1 & 0 & 1 & 0 \end{bmatrix}, \begin{bmatrix} 0 & 0 & 1 & 1 & 1 \\ 1 & 0 & 0 & 1 & 0 \\ 0 & 1 & 0 & 0 & 0 \end{bmatrix}, \begin{bmatrix} 0 & 0 & 1 & 1 & 1 \\ 0 & 1 & 0 & 1 & 0 \\ 1 & 0 & 0 & 0 & 0 \end{bmatrix}, \begin{bmatrix} 0 & 0 & 1 & 1 & 1 \\ 1 & 0 & 0 & 0 & 0 \\ 0 & 1 & 0 & 0 & 0 \end{bmatrix} \end{array} \right\}. \quad (22)$$

By substituting the traffic volume of each approach carriageway into equation (13), the traffic volume T_V of each phase scheme in p is obtained as

$$\left\{ \begin{array}{l} 4300, 4252, 3821, 3773, 4252, 3821, 3773, 4204, \\ 3773, 3725, 3773, 3725, 3342, 3294, 3294, 3246 \end{array} \right\}. \quad (23)$$

At last, according to Step 9 of the flowchart, adopt the phase scheme with the maximum traffic volume as the final output, which is $\begin{bmatrix} 0 & 0 & 1 & 1 & 1 \\ 1 & 0 & 0 & 1 & 1 \\ 0 & 1 & 0 & 1 & 1 \end{bmatrix}$. Specifically, the first phase is 3, 4, and 5; the second phase is 1, 4, and 5; and the third phase is 2, 4, and 5. The actual signal timing for the above-mentioned phase scheme was obtained by using the Webster method [11]. The results are shown in Figure 5.

In cycle 2, following the above process, the phase scheme with the maximum traffic volume is obtained as $\begin{bmatrix} 0 & 0 & 1 & 1 & 1 \\ 0 & 1 & 0 & 1 & 1 \\ 1 & 0 & 0 & 0 & 1 \end{bmatrix}$. The actual signal timing for the above phase scheme was obtained by using the Webster method. The results are shown in Figure 6.

4.5. Traffic Organization Optimization. Before implementing the optimal phase scheme generated from the proposed model, the traffic organizations at the target roundabout need to be adjusted accordingly.

(1) The circulating lane signal is removed

(2) The circulating lane markers are also changed accordingly

The improved traffic organization of the target roundabout is shown in Figure 7.

4.6. Simulation and Performance Comparison. This section simulates and compares the performances of the current signal configuration and the optimized signal scheme for the target roundabout using VISSIM, as shown in Figure 8.

The input traffic volumes, the simulated current, and the simulated optimized traffic volumes of each approach carriageway of the target roundabout are summarized in Table 7.

5. Results and Discussion

Three common intersection evaluation indicators including average queue length, average number of stops, and average delay are adopted for performance comparison. After the

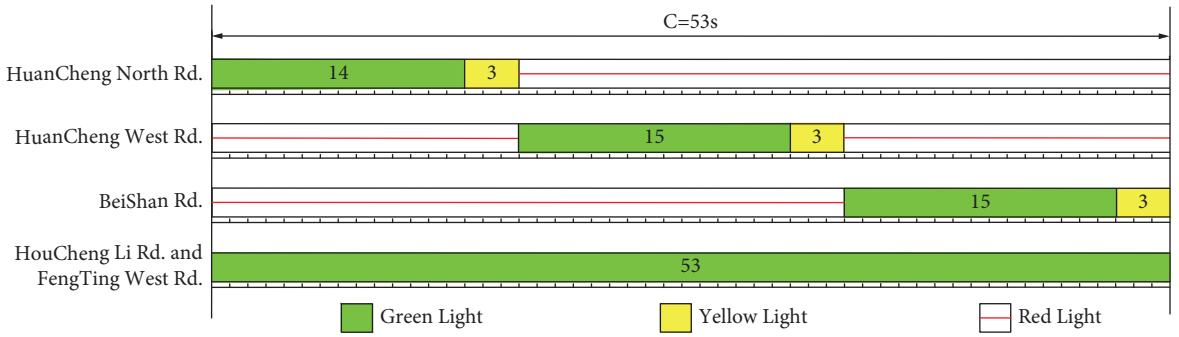

Figure 5: Optimized signal timing in cycle 1 for the model output scheme.

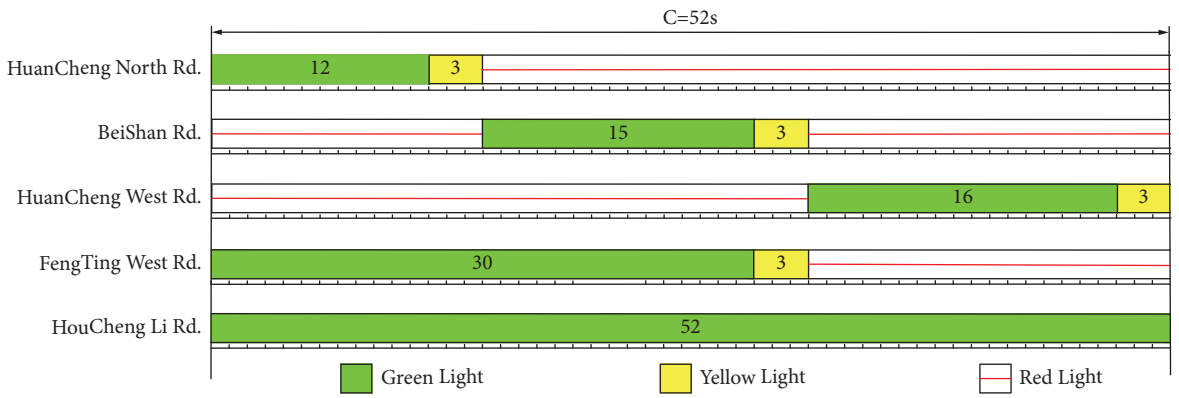

Figure 6: Optimized signal timing in cycle 2 for the model output scheme.

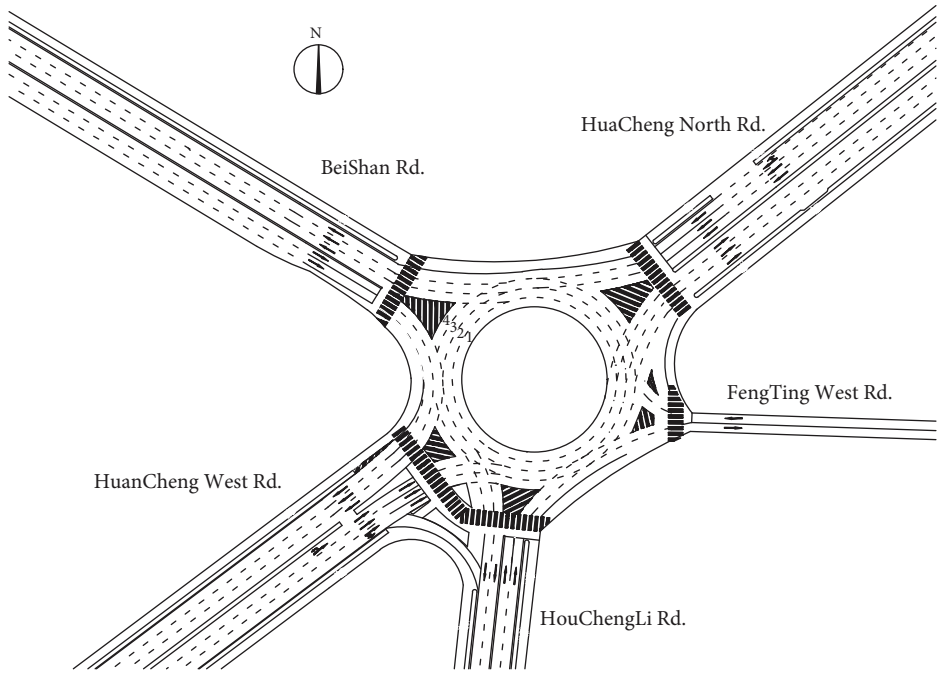

Figure 7: Optimized traffic organization of the target roundabout.

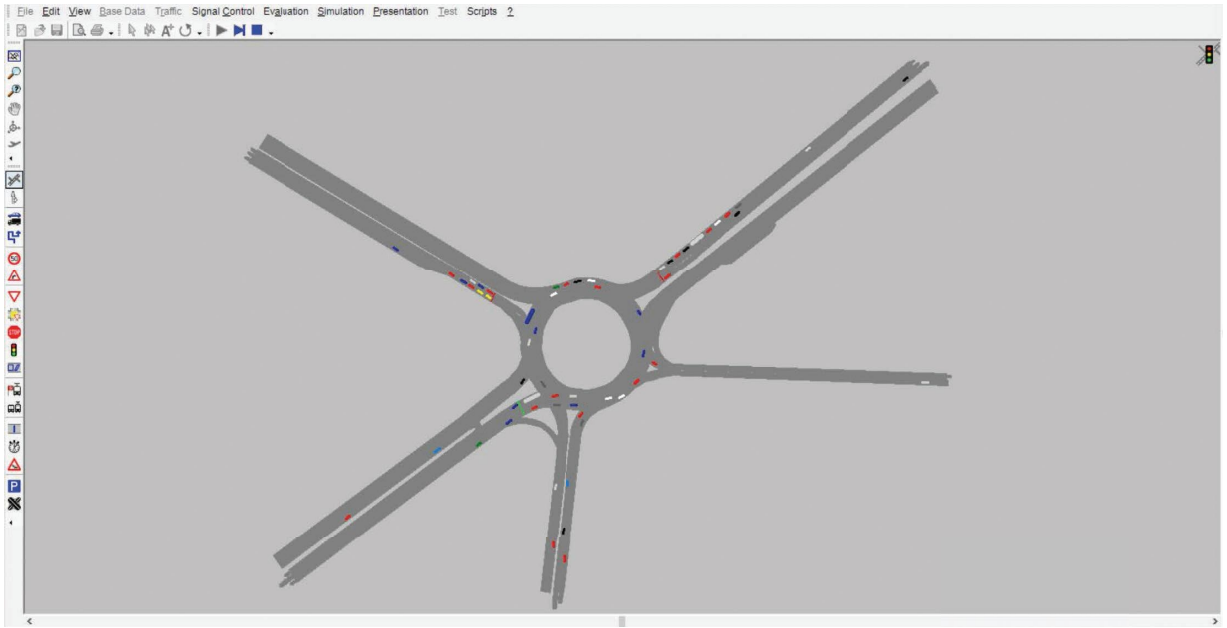

Figure 8: Simulation and comparison of the target roundabout performances using VISSIM.

Table 7: The input and simulated traffic volumes for each approach carriageway (veh).

Approach no.	Cycle no.	1	2	3	4	5	Sum
Input	1	991	726	1002	28	479	3246
	2	1093	717	884	24	453	3171
Current	1	897	704	945	18	412	2976
	2	974	698	801	17	389	2879
Optimized	1	869	710	957	19	446	3001
	2	983	711	846	20	405	2965

Table 8: Performance comparison results in cycle 1.

Approach no.	Average queue length (m)		Average number of stops (times)		Delay (*s*)	
	Current	Optimized	Current	Optimized	Current	Optimized
1	39.0	42.2	0.38	0.44	22.4	29.9
2	26.1	23.4	1.33	0.91	36.3	32.5
3	67.3	45.3	1.29	0.89	45.8	34.1
4	0.6	0.1	0.23	0.10	27.1	11.2
5	19.2	9.7	0.43	0.21	38.0	19.1
Mean	30.4	24.1	0.73	0.51	35.3	30.1

Table 9: Performance comparison results in cycle 2.

Approach no.	Average queue length (m)		Average number of stops (times)		Delay (*s*)	
	Current	Optimized	Current	Optimized	Current	Optimized
1	44.3	46.5	0.41	0.45	24.8	30.6
2	25.5	23.2	1.25	0.90	34.1	28.9
3	60.2	39.6	1.22	0.86	41.1	32.3
4	0.5	0.1	0.20	0.11	25.3	10.7
5	18.3	9.6	0.38	0.19	32.5	17.5
Mean	29.8	23.8	0.69	0.50	32.6	28.8

VISSIM simulation, the corresponding performance comparison results are shown in Tables 8 and 9. In addition, the average queue length and the average number of stops are used as arithmetic means to calculate the mean values, while the mean value of the average delay is obtained based on the following equation:

$$\Omega = \frac{\sum_{i=1}^{N} d_i e_i}{\sum_{i=1}^{N} e_i}, \tag{24}$$

where Ω is the mean value of the average delay (s); d_i refers to the average delay of the approach carriageway i (s); e_i is the $s_i\Omega$ simulated traffic volume of the approach carriageway i (veh).

By comparing the simulation result of the current configuration with that of the optimized configuration, the following conclusions can be drawn:

(1) In cycle 1 and cycle 2, the average queue length of the target roundabout was reduced by 20.72% and 20.13%, respectively. In cycle 1, the Huan-Cheng West Rd. is the only exception where the queue length has slightly increased by 3.2 m due to the conflict between vehicles entering from Huan-Cheng West Rd. and vehicles exiting to Hou-Cheng-Li Rd., which is why the average queue length at the Huan-Cheng West Rd. also increased in cycle 2. Beyond that, the average queuing length of all other approach carriageways has been substantially reduced.

(2) In cycle 1 and cycle 2, the average number of stops at the target roundabout has been substantially reduced by 30.14% and 27.54%, respectively. The only exception is still the average number of stops at Huan-Cheng West Rd., which has increased by only 0.06 in cycle 1 and 0.04 in cycle 2 due to the aforementioned vehicle movement conflicts.

(3) In cycle 1 and cycle 2, the average delay at the target roundabout has been reduced by 14.73% and 11.66%, respectively. Similarly, the only exception is the delay at Huan-Cheng West Rd. which has increased by 7.5 s in cycle 1 and 5.8 s in cycle 2. Apart from the optimized signal scheme generated by the proposed model, the cancellation of traffic lights in the circulating lanes may also contribute to the average delay reduction since the traffic flows in the circulating lanes no longer need to slow down or stop to wait for the green time.

Based on the actual traffic demand during the morning peak period (7:00 to 9:00), the combined phase design model can be used to calculate the capacity of each bottleneck area (especially the B_1 area) and the geometric characteristics of the target roundabout and transform the current dual signal control into a single signal control to make the phase scheme more suitable for the actual traffic conditions, which is the reason the performances of the target roundabout in terms of all three indicators have been greatly improved. In other words, the optimized phase scheme was proved feasible, and the traffic efficiency of the roundabout was substantially increased. Therefore, the combined phase design model can indeed improve the current unreasonable phase setting at many multileg roundabouts by adapting to real-time traffic flow fluctuations.

Pedestrian crossing situation: the sidewalks are equipped with stop signs, which affect the traffic flow inside the roundabout to varying degrees. When a small number of pedestrians conflict with the traffic flow, the proposed approach can still have satisfactory performances. If the number of pedestrians further increases, the conflict between pedestrians and traffic flow will cause additional delays, resulting in the change of road capacity, and the model performances will be inevitably compromised.

6. Conclusions

This paper proposed a combined phase design model to optimize the signal control at multileg roundabouts with the aim of achieving the maximum utilization of roundabout capacity, resulting in the following conclusions:

(1) The proposed combined phase design model for the multileg roundabout is developed based on the traffic operation characteristics and the capacity of each area of the roundabout.

(2) The proposed model is validated by the case of the Hou-Cheng-Li Rd./Bei-Shan Rd. Roundabout to Jinhua. Experimental results indicate that the combined phase design model can reduce the average queue length, the average number of stops, and the average delay by 20.72%, 30.14%, and 14.73% in cycle 1, respectively, and in cycle 2, the three metrics are reduced by 20.13%, 27.54%, and 11.66%, respectively. Thus, the proposed model can effectively improve the traffic efficiency of the roundabout.

(3) Furthermore, this model can be used in actuated signal control to better cope with the real-time traffic demands at roundabouts. Thus, it can contribute to a better control effect in green wave control and area control for roundabouts with unstable traffic.

At last, it is also worth noting that this paper only studies motor vehicle traffic flow and does not consider the impact of mixed traffic flows. In other words, the proposed model cannot be used to solve the optimal phase schemes when roundabout pedestrian traffic flow is involved. In addition, the proposed model is only applicable to cases where excessive traffic delays at roundabouts are caused by large traffic volumes (but still below roundabout capacity). If the traffic volume is small, the roundabout does not need any signal control. On the other hand, the roundabout should be reconstructed if the traffic volume is even larger than its capacity. As such, future research directions include improving the combined phase design model to further solve the pedestrian crossing safety and efficiency issues at roundabouts and to study the phase optimization and signal timing problems of multileg intersections other than roundabouts.

Data Availability

Data cannot be shared publicly because of the confidentiality requirements of the Traffic Police Brigade of Jinhua, Zhejiang, China, who imposed data sharing restrictions on the data underlying our study. Data are only available for researchers who meet the criteria for access to confidential data.

Conflicts of Interest

The authors declare that they have no conflicts of interest.

Authors' Contributions

Cheng-yuan MAO designed the study; Qin WANG conducted data analysis and wrote the report: Wen-jiao XU and Sheng-de YANG collected the data; Xin CHENG and Pei-ran LI contributed to the rationale and discussion of the results. All authors have read and agreed to the published version of the manuscript.

Acknowledgments

This research was funded by the Project of Science and Technology of the Jinhua, China (2021-4-376) and the Project of Science and Technology of the Jinhua, China (2021-4-376) and the Natural Science Foundation of Zhejiang Province (LY18G030021).

References

[1] Z. W. Qu, Y. Z. Duan, X. M. Song, and X. Yan, "Review and outlook of roundabout capacity," *Journal of Transportation Systems Engineering and Information Technology*, vol. 14, no. 5, pp. 15–22, 2014.

[2] X. T. Sun, W. J. Ma, and H. Wei, "Comparative study on the capacity of a signalized roundabout," *IET Intelligent Transport Systems*, vol. 10, no. 3, pp. 307–323, 2016.

[3] R. Rossi, C. Meneguzzer, F. Orsini, and M. Gastaldi, "Gap-acceptance behavior at roundabouts: validation of a driving simulator environment using field observations," *Transportation Research Procedia*, vol. 47, pp. 27–34, 2020.

[4] H. F. Jia and B. L. Li, "Calculation of traffic capacity at signalized roundabouts based on gap acceptance theory," *Journal of Transport Information and Safety*, vol. 36, no. 3, pp. 67–71, 2018.

[5] H. M. N. Al-Madani, "Capacity of large dual and triple-lanes roundabouts during heavy demand conditions," *Arabian Journal for Science and Engineering*, vol. 38, no. 3, pp. 491–505, 2012.

[6] W. Ting, J. L. Grenard, and H. R. Shah, "Developing capacity models for local roundabouts, a streamlined process," *Journal of the Transportation Research Board*, vol. 2257, pp. 1–9, 2011.

[7] Y. Wu, D. Z. Wang, and F. Zhu, "Influence of CAVs platooning on intersection capacity under mixed traffic," *Physica A: Statistical Mechanics and Its Applications*, vol. 593, Article ID 126989, 2022.

[8] J. G. Wardrop, "The Traffic Capacity of Weaving Sections of roundabouts," in *Proceedings of the First International Conference on Operational Research*, Oxford English University Press, Oxford, UK, 1957.

[9] T. N. Chun and W. Heng, "Optimizing actuated traffic signal control using license plate recognition data: methods for modeling and algorithm development," *Transportation Research Interdisciplinary Perspectives*, vol. 9, Article ID 100319, 2021.

[10] K. Lu and G. R. Lin, "Intersection split allocation model considering traffic flow demand," *Journal of Southeast University (Natural Science Edition)*, vol. 49, no. 3, pp. 603–610, 2019.

[11] W. Cheng, X. Liu, and J. M. Lei, "Optimization of cycle of intersection signal based on RBF neural network prediction," *Journal of Chongqing Jianzhu University*, vol. 40, no. 4, pp. 13–18, 2021.

[12] L. Xiao (Joyce), S. I. Guler, and V. V. Gayah, "Decentralized arterial traffic signal optimization with connected vehicle information," *Journal of Intelligent Transportation Systems*, 2022.

[13] W. Ma, L. Wan, C. Yu, L. Zou, and J. Zheng, "Multi-objective optimization of traffic signals based on vehicle trajectory data at isolated intersections," *Transportation Research Part C: Emerging Technologies*, vol. 120, Article ID 102821, 2020.

[14] M. J. S. Shiri and H. R. Maleki, "Maximum green time settings for traffic-actuated signal control at isolated intersections using fuzzy logic," *International Journal of Fuzzy Systems*, vol. 19, no. 1, pp. 247–256, 2017.

[15] W. Ma, Y. Liu, L. Head, and X. Yang, "Integrated optimization of lane markings and timings for signalized roundabouts," *Transportation Research Part C: Emerging Technologies*, vol. 36, no. 11, pp. 307–323, 2013.

[16] X. C. Jiang, L. Y. Zhong, and S. Gao, "Design and signal control method for waiting areas of roundabout," *China Journal of Highway and Transport*, vol. 33, no. 5, pp. 143–152, 2020.

[17] H. Wang, G. X. Peng, and X. G. Yang, "The relationship between traffic signal phasing-sequence and intersection geometry design," *Journal of Highway and Transportation Research and Development*, vol. 21, no. 2, pp. 92–94, 2004.

[18] J. Wu, P. Liu, X. Qin, H. Zhou, and Z. Yang, "Developing an actuated signal control strategy to improve the operations of contraflow left-turn lane design at signalized intersections," *Transportation Research Part C: Emerging Technologies*, vol. 104, pp. 53–65, 2019.

[19] X. H. Xia and L. H. Xu, "Negotiation game coordination control between phases at signalized intersection," *Journal of Highway and Transportation Research and Development*, vol. 39, no. 04, pp. 131–139, 2022.

[20] R. Nei and S. J. Ma, "A lane-based optimization model for lane function and signal phase at intersection," *Journal of Tongji University*, vol. 48, no. 05, pp. 683–693, 2020.

[21] G. Shen, X. Zhu, W. Xu, L. Tang, and X. Kong, "Research on phase combination and signal timing based on improved K-medoids algorithm for intersection signal control," *Wireless Communications and Mobile Computing*, vol. 2020, Article ID 3240675, pp. 1–11, 2020.

[22] Z. Liang, Y. Xiao, and Y.-P. Flötteröd, "An overlapping phase approach to optimize bus signal priority control under two-way signal coordination on urban arterials," *Journal of Advanced Transportation*, vol. 2021, Article ID 6624130, 13 pages, 2021.

[23] X. C. Jiang, Y. Jin, and Y. L. Ma, "Dynamic phase signal control method for unstable asymmetric traffic flow at intersections," *Journal of Advanced Transportation*, vol. 2021, Article ID 8843921, 16 pages, 2021.

[24] P. Han, *Operation Characteristics of Traffic Flow at Roundabout*, Jilin University, Changchun, China, 2011.

[25] J. Q. Xu, *Introduction to Traffic Engineering*, pp. 94–100, China Communications Press, BEIJING, 2008.

[26] W. L. Jin, "A kinematic wave theory of lane-changing traffic flow," *Transportation Research Part B:Methodological*, vol. 44, no. 8-9, pp. 1001–1021, 2010.